Recovery of PMOSFET NBTI under different conditions*

Cao Yan-Rong(曹艳荣)[a)b)†], Yang Yi(杨 毅)[a)], Cao Cheng(曹 成)[a)], He Wen-Long(何文龙)[a)], Zheng Xue-Feng(郑雪峰)[b)], Ma Xiao-Hua(马晓华)[c)], and Hao Yue(郝 跃)[b)]

[a)] *School of Mechano-electric Engineering, Xidian University, Xi'an* 710071, *China*
[b)] *Key Laboratory of Wide Band-gap Semiconductor Materials and Devices, School of Microelectronics, Xidian University, Xi'an* 710071, *China*
[c)] *School of Technical Physics, Xidian University, Xi'an* 710071, *China*

(Received 9 July 2014; revised manuscript received 1 April 2015; published online 10 July 2015)

Negative bias temperature instability (NBTI) has become a serious reliability issue, and the interface traps and oxide charges play an important role in the degradation process. In this paper, we study the recovery of NBTI systemically under different conditions in the P-type metal–oxide–semiconductor field effect transistor (PMOSFET), explain the various recovery phenomena, and find the possible processes of the recovery.

Keywords: negative bias temperature instability (NBTI), P-type metal–oxide–semiconductor field effect transistor, recovery

PACS: 73.40.Qv, 85.30.Tv **DOI:** 10.1088/1674-1056/24/9/097304

1. Introduction

Negative bias temperature instability (NBTI) is a crucial reliability issue affecting the P-type metal–oxide–semiconductor field effect transistor (PMOSFET) with a negative voltage stress on the gate at high temperature.[1–5] NBTI causes an increase of the threshold voltage $V_{\rm th}$ and a decrease of the drive current $I_{\rm d}$ with time, and the parameters shift further at higher temperature and under stronger gate stress. In the conventional NBTI study, the device is stressed by a constant negative gate bias with its drain and source grounded.[6–8] However, the NBTI degradation substantially recovers after the remove of the stress or under a smaller gate bias. Therefore, the conventional stress overestimates the degradation and underestimates the lifetime of the device.[9,10] More attention has been paid to this problem in recent years.[11–13] However, in spite of the intensive studies on the recovery issue, the physical mechanism is still far from being fully understood. In this paper, we study the recovery of NBTI systemically under different conditions in the 90-nm PMOSFETs, explain the various recovery phenomena, and find the possible processes of the recovery.

2. Devices and experiments

The PMOSFETs used here are of the surface channel. They were manufactured by using a 90-nm process technology and had lightly doped drain (LDD) structures and shallow trench isolation (STI) schemes. The devices were 0.1 μm in length, 10 μm in width, and 1.4 nm in oxide thickness. The gate oxides of all devices were annealed in N_2O atmosphere after thermal growth. HP 4156B, a high precision semiconductor parameter analyzer, was used to complete the tests. The devices were stressed under NBTI stress conditions of $V_{\rm g} = V_{\rm stress}$ and $V_{\rm d} = V_{\rm s} = 0$ at elevated temperatures for different cycles. The stress was interrupted at regular intervals, and the device parameters such as threshold voltage $V_{\rm th}$ were measured to monitor the degradation of the device. After the stress process, the recovery process was studied under different gate biases at different temperatures.

3. Results and discussion

To study the recovery mechanism, experiments were carried out to obtain the results of different recovery processes under different gate biases at different temperatures. As the threshold voltage $V_{\rm th}$ is one of the most important parameters, the difference between the initial $V_{\rm th}$ indicated by $V_{\rm th0}$ and $V_{\rm th}$ ($\Delta V_{\rm th}$) was measured at the stress intervals. The $V_{\rm th}$ degradation was studied and its mechanism was analyzed.

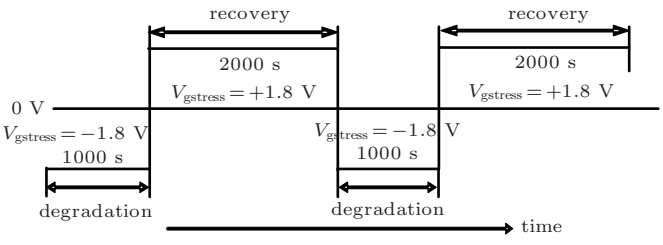


Fig. 1. The applied alternating stress.

*Project supported by the National Basic Research Program of China (Grant No. 2011CBA00606), the National Natural Science Foundation of China (Grant Nos. 61404097, 61334002, 61106106, and 61176130), and the Fundamental Research Funds for the Central Universities, China (Grant No. JB140415).

†Corresponding author. E-mail: yrcao@mail.xidian.edu.cn

© 2015 Chinese Physical Society and IOP Publishing Ltd

The applied alternating stress is shown in Fig. 1. The negative bias $V_{\rm gstress} = -1.8$ V is applied during the degradation process, and the positive bias $V_{\rm gstress} = +1.8$ V is applied during the recovery process. In order to study the recovery mechanism, the recovery process lasts 2000 s, while the degradation process lasts 1000 s. Suppose that the last $\Delta V_{\rm th}$ of each negative bias stress cycle is $\Delta V_{\rm th}^0$. We will plot different recovery cycles with the values of $\Delta V_{\rm th}/\Delta V_{\rm th}^0$ in the same time scope under different conditions.

3.1. Recovery of different cycles

In the NBTI degradation process, in addition to the interface trap generation, there are also generated H related species including H^+.[14] The H related species are easily trapped by the oxide traps during migrating to the gate. Furthermore, during the NBTI stress, a large number of inversion holes gather at the channel surface, and some of them can tunnel into the gate oxide and be trapped by the oxide traps. Therefore, when the negative gate stress is instantly removed, in addition to the H related species, there are also a number of positive charges in the oxide. The H related species and the positive charges can play a role in recovering NBTI. Figure 2 is the species distribution in the gate oxide under the NBTI stress.

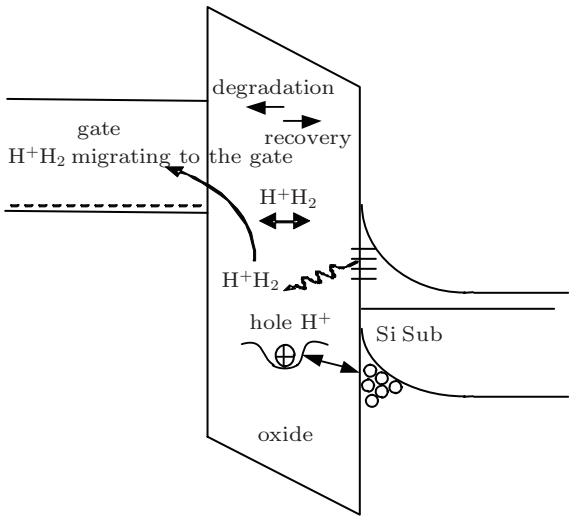


Fig. 2. Relevant species distribution in the gate oxide in the NBTI degradation process. Here ⊕ represents positive charges trapped in the oxide, ◯ represents inversion holes.

To study the recovery mechanism, we use a longer recovery time, and the variation of the threshold voltage under the applied alternating stress is shown in Fig. 3. We study the recovery and degradation stages in detail.

The threshold voltage shifts of two recovery cycles are given in Fig. 4(a). The actual time range of the first recovery cycle is 1000–3000 s, and that of the second recovery cycle is 4000–6000 s. The markings are the degradation quantities of the degradation phases ahead of the two recovery cycles separately. As shown in Fig. 4, the recovery process can be divided into three stages: the stage marked by 1 is the first recovery stage, results from the detrapping of the oxide charges, and is the fast recovery stage; the stage marked by 2 is the second recovery stage due to the passivation of the interface traps by the H related species, and is the slow recovery stage; the stage marked by 3 is the third recovery stage and is the recovery saturation stage. In both the degradation and the recovery processes, there are H related species entering into the gate. Therefore, the H related species moving back and passivating the interface traps are reduced. The final recovery amount is smaller than the degradation, and the lock-in effect of part degradation or the recovery saturation stage comes out.[15]

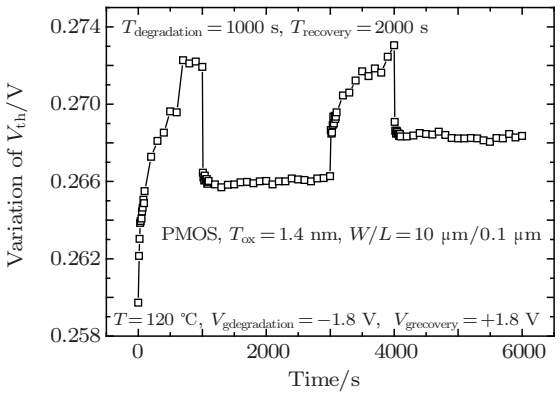


Fig. 3. Time variation of threshold voltage under the alternating stress.

It is clear that the threshold voltage degradation after recovery of the second cycle is far larger than that of the first cycle. Mark the last points of the degradations as $\Delta V_{\rm th}^0$. Through the normalized processing, we can see that the total threshold voltage degradation increases after the recovery of the second cycle, as shown in Fig. 4(b). Similarly, after being normalized, the recovery of each recovery cycle marked as $\Delta V_{\rm th-Recovery}$ is compared with the final degradation after the previous degradation process in Fig. 4(c), which shows that the recovery of the second cycle is much smaller than that of the first cycle.

The above results are all about degradation comparison between different cycles. Actually, the total degradation after the second cycle minus the final value of the first cycle is the real degradation during the second cycle. By comparing the ratio between the recovery after the recovery process and the real degradation of each cycle marked as $\Delta V_{\rm th-Degradation}$, we find that the recovery ratio of the second cycle is larger than that of the first cycle as shown in Fig. 4(d). Therefore, the reason why the final degradation of the recovery stage increases with cycle number increasing is not the decrease of recovery during each cycle, but the accumulation of recovery saturation during the recovery stage of each cycle.

From Fig. 4, we can clearly see that the final recovery is almost determined by the fast recovery stage. Namely, the detrapping of the gate oxide positive charges is the key. In addition, figure 4(d) shows that as the number of cycles increases, the effect of the detrapping of gate oxide positive charges is more significant.

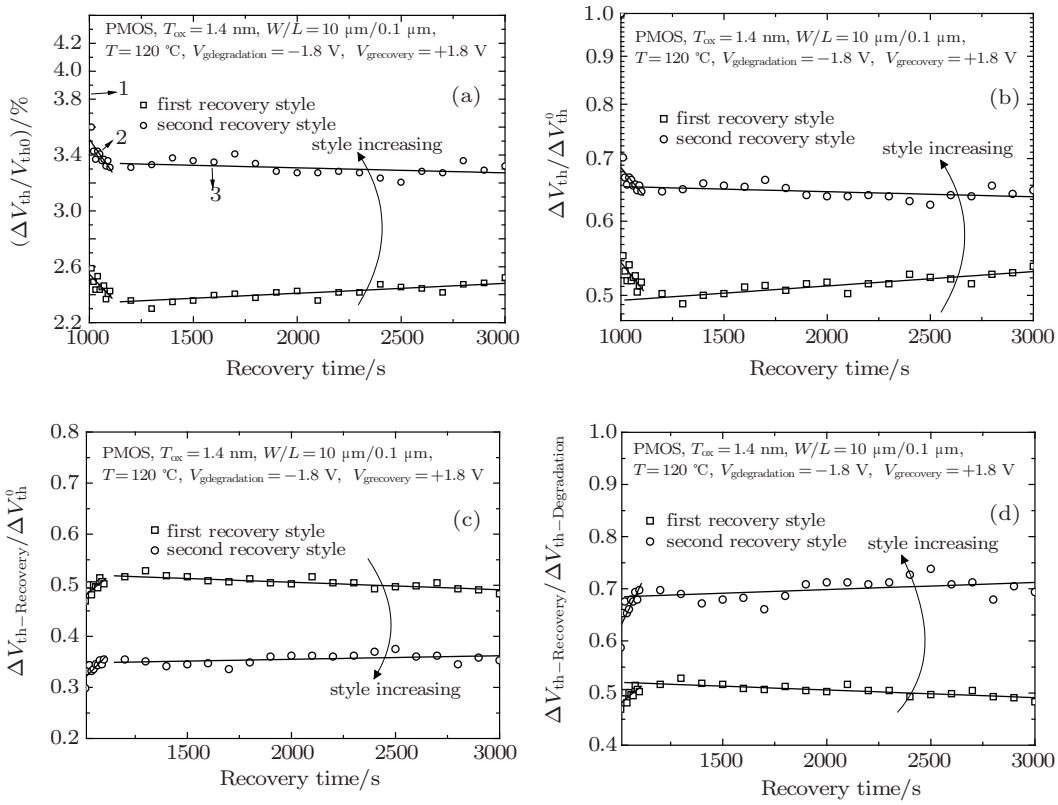


Fig. 4. Recovery stages of NBTI: (a) the superposition of threshold voltage shifts of two recovery cycles, (b) the normalized superposition of the final threshold voltage degradation after recovery relative to that after the previous degradation process, (c) the normalized superposition of the threshold voltage recovery after the recovery stage relative to the final degradation after the previous degradation process, (d) the superposition of the threshold voltage recovery after the recovery stage to the real degradation of this cycle ratio.

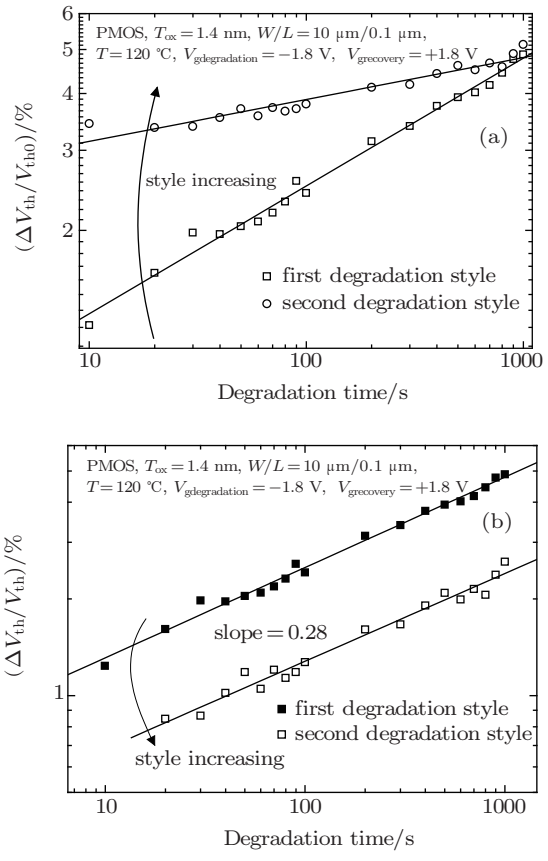


Fig. 5. Two cycles of NBTI degradation stages: (a) the device threshold voltage shifts and (b) the normalized threshold voltage shifts.

The threshold voltage shifts of the two cycles in the NBTI degradation stress processes are shown in Fig. 5(a). The actual time range of the first degradation process is 0–1000 s, and that of the second degradation process is 3000–4000 s. On the whole, the degradation rate of the second process is far smaller than that of the first process. We consider the second degradation stage as an independent process, the threshold voltage shift relative to the end point of the first recovery stage is shown in Fig. 5(b). It is clear that the time exponent of the second stage is the same as that of the first stage, both stages meet the same degradation model, i.e., the H–H^{+} reaction diffusion model.[16]

3.2. Recovery at different temperatures

Figure 6 shows the recovery of the threshold voltage during the recovery stage at different temperatures. We can clearly see that the recovery decreases obviously when the temperature increases from 90 °C to 150 °C. This is because during the degradation of NBTI, the temperature plays an important role in the interfacial reaction and the reaction products' diffusion to the gate oxide. Si–H bond breaking, which is a forward electrochemical reaction, is an endothermic process. The backward reaction, or the passivation reaction of the interface traps, is an exothermic process. The high temperature promotes the forward and the backward reactions to different degrees, disequilibrates the forward and the back-

ward reactions, and relatively limits the passivation reaction rate. Hence, more H related species are produced with temperature rising. Meanwhile, the energy of the charged particle increases, which reduces the probability of the charged particles being trapped by the gate oxide traps. More H related species can enter into the ploy-Si gate, so the number of positive charges and that of the H related species which can diffuse back to the interface to passivate the interface traps become smaller. It eventually leads to the reduced device recovery at high temperature. Therefore, high temperature will solidify the damages of the gate oxide, shown as recovery saturation or a lock-in effect, which can enhance device damages.

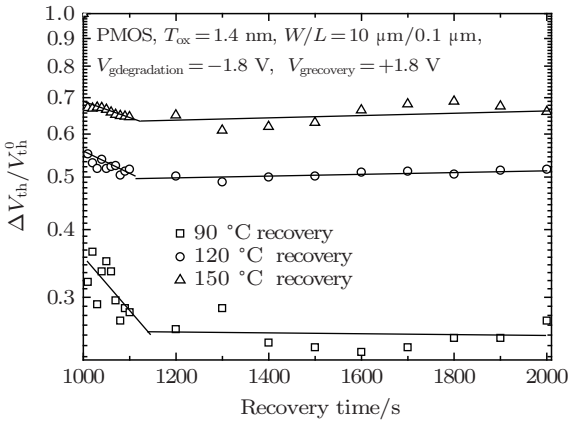


Fig. 6. Normalized threshold voltage recovery at different temperatures.

We can respectively obtain the recovery of the first and the second recovery stages from Fig. 6, corresponding to fast detrapping and passivation of the interface traps. Their relations to temperature are shown in Fig. 7. In the single logarithmic coordinate, they both show good linear relations with $1/KT$ and satisfy the equation

$$R_1 = \Delta(\text{recovery})/\Delta^0 = C\exp(E_a'/KT), \tag{1}$$

where R_1 is the ratio between the normalized recovery $\Delta(\text{recovery})$ and the initial degradation Δ^0, C is a constant, K is the Boltzmann constant, T is the absolute temperature, and E_a' is the relation factor. This equation has the same form as the Arrhenius equation,[17] but the relation between variable and independent variable is inverse. Here, the recovery increases with temperature reducing, or $\Delta \sim 1/KT$, but the relation in the Arrhenius equation is $\Delta \sim -1/KT$. Therefore, the relation factor also shows the activation made by temperature for device recovery, named the activation energy. Meanwhile, we find that the activation energy corresponding to oxide charges or the fast recovery stage is about 0.145 eV, and that corresponding to interface traps passivation or the slow recovery stage is about 0.508 eV. It explains that the interface trap passivation is much more difficult than oxide charge detrapping.

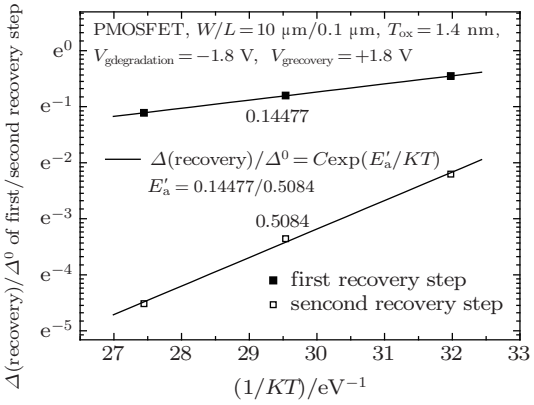


Fig. 7. Variations of the first and the second recovery stage with temperature.

Taking both recovery factors into account, we obtain the final device recovery as shown in Fig. 8. In the single logarithmic coordinate, the final recovery still shows an obvious linear relation with $1/KT$ and meets the following equation:

$$R_2 = \Delta V_{\text{th-Recovery}}/\Delta V_{\text{th}}^0 = C\exp(E_a'/KT), \tag{2}$$

where R_2 is the ratio between the normalized recovery quantity $\Delta V_{\text{th-Recovery}}$ and the initial degradation quantity ΔV_{th}^0, and E_a' is between the previous two values, a value of 0.173 eV is obtained in the experiment. So we obtain the final degradation

$$\Delta V_{\text{th}} = \Delta V_{\text{th}}^0(1-R_2) = \Delta V_{\text{th}}^0[1-C\exp(E_a'/KT)]. \tag{3}$$

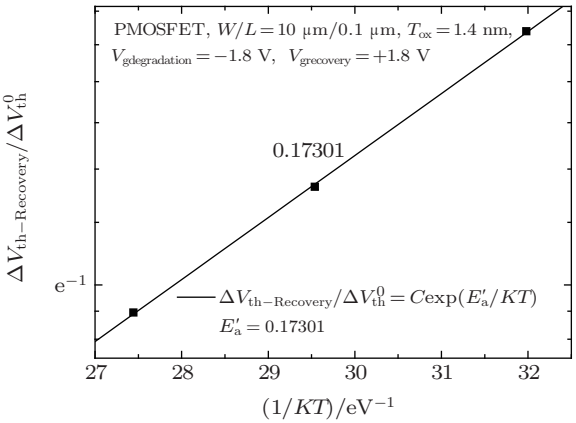


Fig. 8. Dependence of total recovery on temperature during the recovery stage.

3.3. Recovery under different recovery stresses

In the recovery process, the recovery of the NBTI effect differs under different recovery stress. Figure 9 shows the recovery of the threshold voltage under different gate biases. As shown in the figure, the recovery process can be divided into three stages and the recovery keeps increasing with the recovery stress varying from 0 V to 1.8 V. From the experimental results, we can obtain the reason why the recovery is mainly determined by the different fast recovery in the recovery stage. Higher recovery gate stress will lead to more gate

oxide charges, which affects the device recovery. Besides, the high gate voltage can also facilitate the H^+ ions to diffuse back to the Si/SiO_2 interface to passivate the interface traps in a short time. So the larger fast recovery is produced.

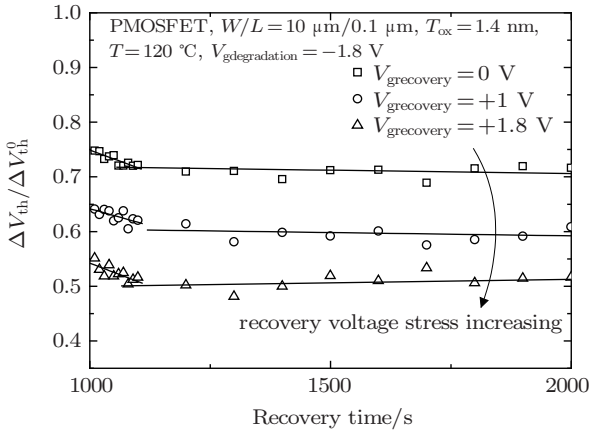


Fig. 9. Normalized V_{th} recovery under different recovery gate biases.

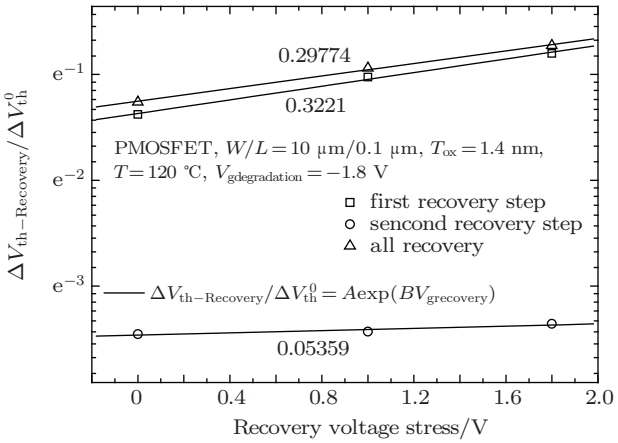


Fig. 10. Variations of recovery during each stage under different recovery gate stresses.

We extract the respective and the total amount of recovery, as shown in Fig. 10. It shows the obvious dependence of recovery after NBTI stress on the gate bias. All three kinds of recovery present good linear relations with the recovery gate bias. The total recovery meets the following equation:

$$R=\Delta V_{th-Recovery}/\Delta V_{th}^0=A\exp(BV_{grecovery}), \quad (4)$$

where R is the ratio between normalized recovery $\Delta V_{th-Recovery}$ and the initial degradation ΔV_{th}^0, A is constant, and B is the relation factor. The factor corresponding to oxide charge detrapping or the fast recovery stage is approximately 0.322, and that corresponding to the interface trap passivation or the slow recovery stage is approximately 0.054. It shows that the first recovery stage is more seriously affected by the recovery gate stress than the second recovery stage, because the first stage is principally caused by gate oxide positive charge detrapping. In the single logarithmic coordinate, the relation between the final recovery and the recovery gate stress is linear, and the relation factor is about 0.298. Hence, we obtain

$$\Delta V_{th}=\Delta V_{th}^0(1-R)=\Delta V_{th}^0[1-A\exp(BV_{grecovery})]. \quad (5)$$

4. Conclusion

By the analyses of recovery under different conditions, we find that gate oxide charge detrapping plays an important role in the device recovery. The device recovery is incomplete, and finally, recovery saturation occurs. The final degradation is closely related to the recovery stress and temperature. High positive recovery gate stress and low temperature are beneficial to the recovery of the NBTI effect.

References

[1] Lu D, Ruggles G A and Wortman J J 1988 *Appl. Phys. Lett.* **52** 1344
[2] Blat C E, Niconlian E H and Poindexter E H 1991 *J. Appl. Phys.* **69** 1712
[3] Maeda S, Maegawa S and Ipposhi T 1994 *J. Appl. Phys.* **76** 8160
[4] Huard V, Denais M and Parthasarathy C 2006 *Microelectronics Reliability* **46** 123
[5] Kushida-Abdelghafar K and Watanabe K 2002 *Apply. Phys. Lett.* **81** 4362
[6] Tsetseris L, Zhou X J, Fleetwood D M, Schrimpf R D and Pantelides S T 2005 *Appl. Phys. Lett.* **86** 142103
[7] Chen C Y, Lee J W and Wang S D 2006 *IEEE Electron Devices* **53** 29933000
[8] Devine R A B, Alshareef H N and Quevedo-Lopez M A 2008 *J. Appl. Phys.* **104** 124109
[9] Ershov M, Saxena S, Karbasi H, Winters S and Minehane S 2003 *Appl. Phys. Lett.* **83** 1647
[10] Chen G, Li M F, Ang C H, Zheng J Z 2002 *IEEE Electron Dev. Lett.* **23** 734736
[11] Yonamoto Y and Akamatsu N 2011 *Appl. Phys. Lett.* **98** 103513
[12] Huang S Y, Chang T C, Yang M C and Lin L W 2012 *Appl. Phys. Lett.* **101** 253502
[13] Nguyen D D, Kouhestani C, Kambour K E and Devin R A B 2014 *J. Vac. Sci. Technol. B* **32** 011205
[14] Krishnan A T, Chakravarthi S, Nicollian P, Reddy V and Krishnan S 2006 *Appl. Phys. Lett.* **88** 153518
[15] Cao Y R, Ma X H, Hao Y, Yu L, Zhu Z W and Chen H F 2007 *Chin. Phys.* **16** 1140
[16] Cao Y R, Ma X H, Hao Y and Tian W C 2010 *Chin. Phys. B* **19** 097306
[17] Alam M A and Mahapatra S 2005 *Micoroelectronics Reliability* **45** 7181